Cell J
Cell Journal(Yakhteh)
Homepage: https://www.celljournal.org/
Original Article
Vol 25, No 6, June 2023, Pages: 407-417

Disulfiram-Loaded Niosomes Reduces Cancerous Phenotypes in Oral Squamous Cell Carcinoma Cells

Melika Zangeneh Motlagh, D.D.S.[1, 2#], Nazanin Mahdavi, D.D.S., M.Sc.[1, 3], Zohreh Miri-Lavasani, M.Sc.[2#], Pouyan Aminishakib, D.D.S., M.Sc.[1, 3], Mahsa Khoramipour, M.Sc.[2], Mandana Kazem Arki, M.Sc.[2], Niloufar Rezaei, M.Sc.[2], Nikoo Hossein-Khannazer, Ph.D.[2], Massoud Vosough, M.D., Ph.D.[4, 5*]

1. Department of Oral and Maxillofacial Pathology, School of Dentistry, Tehran University of Medical Sciences, Tehran, Iran
2. Gastroenterology and Liver Diseases Research Center, Research Institute for Gastroenterology and Liver Diseases, Shahid Beheshti University of Medical Sciences, Tehran, Iran
3. Department of Pathology, Cancer Institute Hospital, IKHC, Tehran University of Medical Sciences, Tehran, Iran
4. Department of Regenerative Medicine, Cell Science Research Center, Royan Institute for Stem Cell Biology and Technology, ACECR, Tehran, Iran
5. Experimental Cancer Medicine, Institution for Laboratory Medicine, Karolinska Institute, Stockholm, Sweden

Abstract

Objective: Surgery and chemotherapy are the most common therapeutic strategies proposed for oral squamous cell carcinoma (OSCC). However, some of the disadvantages associated with the current methods like unwanted side effects and poor drug response lead the scientist to seek for novel modalities and delivery approaches to enhance the efficacy of treatments. The study aimed to assess the effectiveness of disulfiram (DSF)-loaded Niosomes on cancerous phenotypes of the OSCC cells.

Materials and Methods: In this experimental study, an optimum formulation of DSF-loaded Niosomes was developed for the treatment of OSCC cells to reduce drug doses and improve the poor stability of DSF in the OSCC environment. The design expert software was utilized to optimize the particles in terms of size, polydispersity index (PDI), and entrapment efficacy (EE).

Results: Acidic pH increased the release rate of DSF from these formulations. The size, PDI, and EE of Niosomes were more stable at 4°C compared to 25°C. The results indicated that DSF-loaded Niosomes could induce apoptosis (P=0.019) in the OSCC cells compared to the control group. Moreover, it could reduce colony formation ability (P=0.0046) and also migration capacity of OSCC cells (P=0.0015).

Conclusion: Our findings indicated that the application of proper dose of DSF-loaded Niosomes (12.5 µg/ml) increases apoptosis, decreases colony formation capacity and declines the migration ability of OSCC cells.

Keywords: Disulfiram, Drug Delivery, Niosome, Oral Squamous Cell Carcinoma

Citation: **Zangeneh Motlagh M, Mahdavi N, Miri-Lavasani Z, Aminishakib P, Khoramipour M, Kazem Arki M, Rezaei N, Hossein-Khannazer N, Vosough M. Disulfiram-loaded niosomes reduces cancerous phenotypes in oral squamous cell carcinoma cells. Cell J. 2023; 25(6): 407-417. doi: 10.22074/CELLJ.2023.1985869.1202**

Introduction

Lip and oral cavity cancers are the sixth most common type of cancer worldwide with the highest mortality rate and incidence in Asia (1). Among the oral cavity cancers, oral squamous cell carcinoma (OSCC) standing for 90% of tumors affecting this region (2). Based on WHO report in 2020, about 15 million people were diagnosed with this cancer (3). A crucial prognostic factor for oral and oropharyngeal carcinomas is lymph node metastasis. Cervical lymph nodes are the most typical site for OSCC metastasis, and their involvement significantly lowers survival rates (by 50%). On the same side as the original site of the malignancy, cancer cells typically move to the lymph nodes. However, Contralateral or bilateral lymph node metastasesis a rare complication. Carcinomas must undergo specific biological changes in order to spread from the primary tumor location to an anatomically distant region known as distant metastasis. For OSCC, lungs are the most typical location for distant metastases. However, far metastasis to other organs, including bone, liver, and mediastinal nodes were reported. The prognosis is worsened and the likelihood of a successful treatment is decreased by distant metastases. Three important characteristics raise the chance of primary tumor cell's spreading to distant organs, including positive regional lymph node involvement, extracapsular invasion of tumor cells, and lack of human papilloma virus (HPV) (4). However, conventional treatment methods are not completely safe and having their own disadvantages. When undergoing surgery, chemotherapy

Received: 26/December/2022, Revised: 19/April/2023, Accepted: 04/May/2023
#These authors equally contributed to this work.
***Corresponding Address: Department of Regenerative Medicine, Cell Science Research Center, Royan Institute for Stem Cell Biology and Technology, ACECR, Tehran, Iran**
Email: masvos@royaninstitute.org

Royan Institute
Cell Journal (Yakhteh)

and/or radiotherapy, patients suffer from local defects, dysfunctions, drug resistance, and other systemic toxic effects. Considering this fact and the rapid development of genomics, proteomics, metabolomics and biomedical sciences, targeted therapy has become a hot spot in current research. Targeted therapy has the advantage of delivering low toxicity, highly selective and high therapeutic index (5). To achieve better therapy response, new drug delivery systems have been developed. Microparticles, lipid nanoparicles, polymeric nanoparicles, micelles, and nanocrystals have all been used in practical applications of innovative drug delivery systems (6).

Epithelial to mesenchymal transition (EMT) process leading to increased cell motility and invasion, intravasation and extravasation, as well as higher cell survival, speed up the cancer progression. When epithelial cells undergo EMT, expression of mesenchymal markers and matrix metalloproteinases (MMPs) are increased. Epithelial cells lose their cell-adhesive properties, the expression of E-cadherin is suppressed and the invasion and metastatic features of cancer cells are proceeded. Following EMT, a chain of signaling events is set off and a significant remodeling of the cell cytoskeleton occurs. Additionally, during EMT, N-cadherin expression is elevated while E-cadherin expression decreases that makes the cell more motile and invasive. While the cells lose their apical-basal polarity as a result of EMT, they develop a front-back polarity that enables directional cell migration. As a result of increased MMP activity, extracellular matrix proteins were degraded, allowing them to delaminate and escape from their epithelial components (7).

Disulfiram (DSF, Antabuse®) is a drug used for alcohol dependence, however it has wide anticancer characteristics that is suggested to have very promising future in this field of research (6). The anticancer potential of DSF is achieved through blockage of proteasome activity, induction of cell apoptosis, inhibition of invasion and angiogenesis, suppression of stem-like properties, and reduction of drug resistance. It has been proved that DSF suppresses the invasion through inhibition of MMP2 and MMP9. Also in other cancers, particularly breast cancer, tumor growth in a mouse xenograft model was successfully inhibited after application of DSF (8).

In the case of the poor stability of DSF in the gastric environment and its rapid degeneration in the body, development of more effective drug delivery systems is necessary. As an ideal strategy in targeted cancer treatment, nanocarriers could be ideal modalities for targeted and controlled drug release (9). Niosomes are one of the most beneficial and novel drug delivery systems which are biodegradable, quit stable, and non-immunogenic with bilayer structure that enables them for simultaneous delivery of both hydrophobic and hydrophilic drugs (10). Regarding the chemical nature of DSF (poorly water soluble) application of Niosomes enhances stability and limits its side effects in the circulatory system (6). In addition, by increasing the entrapment efficiency and providing continuous release of drugs, it is possible to deliver the appropriate doses of drugs to cancer cells (11).

In this study, we used Niosomes, which are produced when non-ionic surfactants build up in an aqueous media and form a bilayer structure resembling a vesicle. Additionally, they are composed of two parts: a hydrophilic segment and a hydrophobic segment. By enhancing the pharmacokinetics of the pharmaceuticals, the usage of drug-containing Niosomes boosts the therapeutic effects of the drug and lessens its negative effects. Drug stability may potentially be improved as a result of the drug's loading inside the Niosomes (3). Niosomes have physical and chemical characteristics comparable to those of liposomes, with the exception that their permeability for tiny ions/solutes is higher, which could make them appealing as drug carriers or as a platform for delivering a variety of compounds. Niosomes have an advantage over liposomes e.g., their production is remarkably less expensive than phospholipids and both lipids and non-ionic surfactants are equally stable. It was demonstrated that freezing and thawing of them resulted in the loss of potency in Niosomes. Niosomes have been used in preliminary animal trials, but no clinical studies have been reported (12).

The aim of this experimental study is to evaluate the impact of treatment with DSF-loaded Niosomes on cancerous phenotypes of the OSCC cells.

Materials and Methods

Optimization of niosomal formulations using response surface methodology

Through the use of Central Composite design, the response surface methodology (RSM) was employed to optimize niosomal formulations. Two numerical parameters [lipid content (M) and surfactant per cholesterol molar ratio] were chosen to study the impact of their concentration on niosomal particle size (nm), polydispersity index (PDI), and entrapment efficacy percentage (EE%) in order to investigate the relationship between a set of independent and the dependent variables by fitting the data using a polynomial equation. Design-Expert software was used to obtain the polynomial equation (version 7.0.10, Stat-Ease, Inc., Minneapolis, MN, USA). The experimental results and the anticipated reactions were compared. The best formulation was picked for additional investigation using the point prediction approach. These variables and their levels were shown in Table S1 (See Supplementary Online Information at www.celljournal.org).

This study approved by Ethics Committee at Tehran University of Medical Sciences (IR.TUMS.DENTISTRY.REC.1400.015).

Preparation of niosomal formulations

The creation of the Niosomes involved the hydration thin film process. DSF, Span60, and cholesterol were all dissolved in chloroform in precisely the right proportions. To create a thin lipid film, the organic solvent was dried in a rotary evaporator for 30 minutes at 60°C (120 rpm).

The dry films were made Niosomes by adding phosphate buffered saline (PBS, Merck, Germany) to hydrate them. Finally, sonication was used for 5 minutes to produce Niosomes with a consistent size distribution (Hielscher up50H ultrasonic processor, Germany).

Physical characterization of niosomal formulations

Using a tabletop dynamic light scattering (25°C and 633 nm wavelength), the particle size (P=0.00034), zeta potential, and PDI (P=0.0087) of niosomal formulations were assessed (Zetasizer Nano S90, Malvern Panalytical Ltd., Malvern, United Kingdom). The specimens' morphology was examined by using transmission electron microscopy (TEM). On a copper grid with carbon coating, a drop of niosomal formulation was applied before being dyed with 1% phosphotungstic acid. With a TEM (Germany's Zeiss EM900 Transmission Electron Microscope) operating at 100 kV, the thin film of stained Niosomes was photographed (13).

Entrapment efficacy

The niosomal formulations were ultra-filtered using an Amicon Ultra-15 membrane at 4000 rpm for 30 minutes at 4°C in an Eppendorf® 580R centrifuge (Hamburg, Germany). To calculate the entrapment efficacy (EE%), the non-entrapped DSF were divided from the entrapped DSF. Using a UV-visible light spectrophotometer, the absorption at 216 nm was measured to determine the DSF concentration (JASCO, V-530, Japan). The calculated EE% (P=0.0002) was determined using the equation below (14).

$$EE\ (\%) = [(A-B)/A] \times 100$$

A: The initial drugs concentration for niosomal preparation.

B: The concentration of non-entrapped drugs after centrifugation.

In vitro drug release and kinetic study

Two mL of each sample were placed in a semipermeable cellulose acetate dialysis bag to assess the drug release (MWCO 12 kDa). This was submerged in 50 mL of 0.5% w/v PBS-SDS (the releasing medium). The assembly was stirred for 48 hours at 37°C and 50 rpm with a magnetic stirrer under two different pH values (7.4 and 5.4). 1 mL of the released medium was removed and refilled with the same volume of new PBS-SDS at the following times: 1, 2, 4, 8, 24, and 48 hours. Using an ultraviolet light spectrophotometer, it was calculated how much medication was released at predetermined intervals. Using a free drug as a control, the test was performed with equal drug concentrations inside and outside the dialysis bag.

The kinetics of DSF release from the samples were assessed by using a variety of mathematical models, including the Korsmeyer-Peppa's, Higuchi, first-order, and zero-order models (cumulative% drug release vs. time, cumulative% drug remaining vs. time, and cumulative% drug release vs. time) (15). The linear curve was calculated using the correlation coefficient I values that were obtained by regression of the plots acquired from the aforementioned models.

The zero-order model, which describes a system in which the drug release rate is unrelated to concentration, is dependent on drug dissolution. The drug release is described by the first-order rate equation, where the concentration of the medication affects how quickly it is released. The Higuchi and the Korsmeyer-Peppa models show a direct correlation between the amount of drug released from a matrix system and the square root of time (16). Finding the best model for medication release required only a 60% initial release (17).

Cell culture

In this study, primary OCC-11 Cell line was purchased from Iranian Biological Resource Center. It was originally established from a 77-year old man with oral cancer, with prior consent of the doner. Cells were obtained by using enzymatic isolation method (collagenase type I). Then, CD326 (EpCAM) positive cells were isolated by using Magnetic activated cell sorting (MACS) Technology.

Cells were cultured in Dulbecco's Modified Eagle's Medium (DMEM, BioWest, France), F12 supplemented with 10% platelet lysate (pl), 1% penicillin/streptomycin, 1% L-Glutamine, 1% Non-Essential amino acid, 5 µg/ml Hydrocortisone.

Cell viability

The MTT assay was used to measure the viability of cells after drug treatment. Following 24 hours treatment of the cells with DSF-loaded-Niosomes and free DSF (10, 12.5, and 15 µg/ml), PBS washing was performed. Then, MTT solution was added to each well, and the plate was incubated for another 2 hours.

The formed crystals were dissolved in dimethyl sulfoxide (DMSO, Sigma Aldrich, Germany) after the MTT solution withdrawn and purple precipitates have appeared. An Epoch BioTek spectrophotometer plate reader was used to measure the absorbance of the plate at 570 nm. None-treated cells were considered as control group.

Migration assay

The effect of DSF and DSF-Loades Niosomes on the OSCC cell migration was assessed using the wound healing assay. The control groups and the OSCC cells (OCC-11 cell line) were cultivated in 6-well plates and reached to 90% confluence. The scratch was then created with a sterile 100 µl micropipette tip in the middle of the cell monolayer after overnight starvation of the cells. At the specified time (0, 24, 48, and 72 hours) pictures of the wound area were taken in the experimental groups using a microscope (Nikon ECLIPSE Ts2-S-SM). Image J software was utilized to measure the relative migration rate.

Colony formation assay

The OCC-11 cell line was seeded at density of 300 cells/well in a 6-well plate. Following 7-day incubation (37°C, 5% CO_2), the cells were treated with free drug and DFS-loaded Niosomes at determined inhibitory concentration 50 (IC_{50}) concentration for 24 hours. Then, the cells were incubated at 37°C in 5% CO_2 for 14 days, and the culture medium was changed every 2 days. The cells were fixed, and colony morphologies scored. Colonies were fixed with 4% Paraformaldehyde and washed with PBS and then stained with 0.5% crystal violet. A cell colony was defined as a group formation of at least 50 cells and counted using Image J software (National Institutes of Health, Bethesda, Maryland, USA). The surviving fraction for each group was calculated based on the following formula (18).

Plating efficiency (PE) = (Numbler of colonies formed) / (Number of cell seeded)

Surviving fraction (SF) = (Number of colonies formed) / (Number of cell seeded *PE)

Flow cytometry

An Annexin V/PI apoptosis detection kit was used in flow cytometry to assess the distribution of apoptotic cells (BioLegend). Following treatment, the cells were collected and resuspended in 500 µl of stain buffer before being stained for 20 minutes at room temperature in the dark with 5 µl of Annexin V-FITC and 10 µl of PI. BD FACS Calibur (BD Biosiences, San Jose, CA, USA) was used to examine the cells.

Statistical analysis

All the experiments were performed in three biological replicates. The data were analyzed by GraphPad prism software (Version 9.5.1 (528), GraphPad, San Diego, United States of America) and the comparison of difference among experimental groups was done by using one-way ANOVA test. The data are presented as mean ± SEM. $P<0.05$ that was considered as significant.

Results

Formulation of N-DSF

The independent variables in this experiment were the lipid content (M) (A) and the molar ratio of surfactant to cholesterol (B). The responses of nanoparticle size, PDI, EE (%), and release (%) were picked for optimization. The DSF-loaded Niosomes (N-DSF) particle size is in the range of 169.9 to 332.9 nm, according to Table S1A. The response surface plot of the N-DSF particle size is displayed in Figure S1A (See Supplementary Online Information at www.celljournal.org). The particle size grew as the lipid content (M) rose.

Additionally, the size was reduced by raising the molar ratio of surfactant to cholesterol. The PDI for the N-DSF ranges from 0.121 to 0.292, as indicated in Table S1A. The N-DSF PDI response surface map is shown in Figure S1B (See Supplementary Online Information at www.celljournal.org). The PDI initially fell and then climbed as the lipid content (M) was raised. PDI is increased by raising the surfactant to cholesterol molar ratio. The EE (%) of N-DSF from nanoparticles ranges from 51.35 to 84.4%, as shown in Table S1A (See Supplementary Online Information at www.celljournal.org). Figure S1C (See Supplementary Online Information at www.celljournal.org) shows the response surface plot of EE (%) for DSF. EE (%) of DSF decreased as lipid content (M) and the molar ratio of surfactant to cholesterol increased.

Table S1B (See Supplementary Online Information at www.celljournal.org) demonstrates the particle size variance analysis. The response was modeled by a quadratic polynomial ($P\leq0.05$). The model was statistically significant. The amount of lipid present and the surfactant to cholesterol molar ratio both had an impact on particle size. Due to the fitted polynomial responses, the PDI variance analysis demonstrates that the quadratic model is appropriate (Table S1B, See Supplementary Online Information at www.celljournal.org). This statistically significant model ($P\leq0.05$) suggests that PDI is influenced by the molar ratio of surfactant to cholesterol. EE (%) research revealed that 'SF's lipid content and surfactant molar ratio had an impact on EE (%) (Table S1B, See Supplementary Online Information at www.celljournal.org). Table 1 lists the expected models.

Table 1: Predicted models of N-DSF

Particle size (nm)=+204.48+47.77* A-32.10* B-9.78* AB+28.75* A2+22.25* B2
PDI=+0.220+0.008* A+0.022* B+0.062* AB+0.033* A2-0.048* B2
EE (%) of DSF=+71.34105+8.51667* A+9.20333* B+0.462500* AB-5.12263* A2+1.26737* B2

N-DSF; Disulfiram-loaded Niosomes, PDI; Polydispersity index, and EE; Entrapment efficiency.

This model can be used to explore the design space because the signal to noise ratio was determined with adequate precision. All responses met the desired value (ratio greater than 4) (Table 2A). Assessing the model's ability to anticipate outcomes, the Predicted R-squared was calculated. The degree to which the value of R-Squared and Adj R-Squared are similar serves as a gauge of the model's predictive power in this regard. The anticipated R-squared values and the modified R-squared show a reasonable agreement in all replies. The improved formulation was successfully synthesized and characterized in accordance with the desirability criteria (Table 2B). The optimized responses obtained by RSM and the experimental data for the same responses under the optimum conditions presented (Table 2C). The PDI is 0.18', the EE (%) of DSF is 80.1%, and the nanoparticle size is 188.89 nm. By demonstrating the soundness of the optimization plan, the responses were matched to the anticipated response (Table 2D). The optimized formulation was thus employed for additional trials.

Characterization

The particle size of niosomal formulations and empty Niosomes are depicted in Figure 1A and Table S1C (See Supplementary Online Information at www.celljournal.org). The particle size and PDI of the N-DSF were, as can be observed, 189.7 nm and 0.187, respectively. The Niosomes has particles that are 164 nm in size with a PDI of 0.17 (Fig.1B).

Assessing the morphology of ideal Niosomes, TEM was used. The internal structure of the N-DSF is depicted in Figures 1C. In terms of size, N-DSF is about 40 nm. The illustration depicts the two-layered, globular shape of ideal Niosomes. Furthermore, the Niosomes structure's stiff boundaries may be noticed.

Optimization of formulations

Niosome sizes were 189.7 nm (Fig.2A) and 164 nm (Fig.2B), respectively, while the PDI for N-DSF was 0.187 and for an empty Niosome was 0.17. Additionally, empty Niosomes and N-DSF had zeta potentials of -22.6 and -20.4, respectively. The optimized formulations resulted in the right size and homogeneous particle dispersion, according to results related to particle size and PDI.

Drug release study

Diagram of cumulative drug release over time

Figures 1D illustrates the process of DSF's cumulative release over a 48-hour period in PBS containing 0.5% sodium dodecyl sulfate (SDS). Hydrophobic medicines' solubility and stability in buffer medium were improved by using the SDS. Approximately 98.82% of the drug in the case of free DSF is released in the first 8 hours, and then 100% of the drug is released in the next 24 hours. At pH=7.4 in the N-DSF formulation, the drug release of DSF in 48 hours is approximately 56.485%; and at pH=5.4, it is approximately 73.66%.

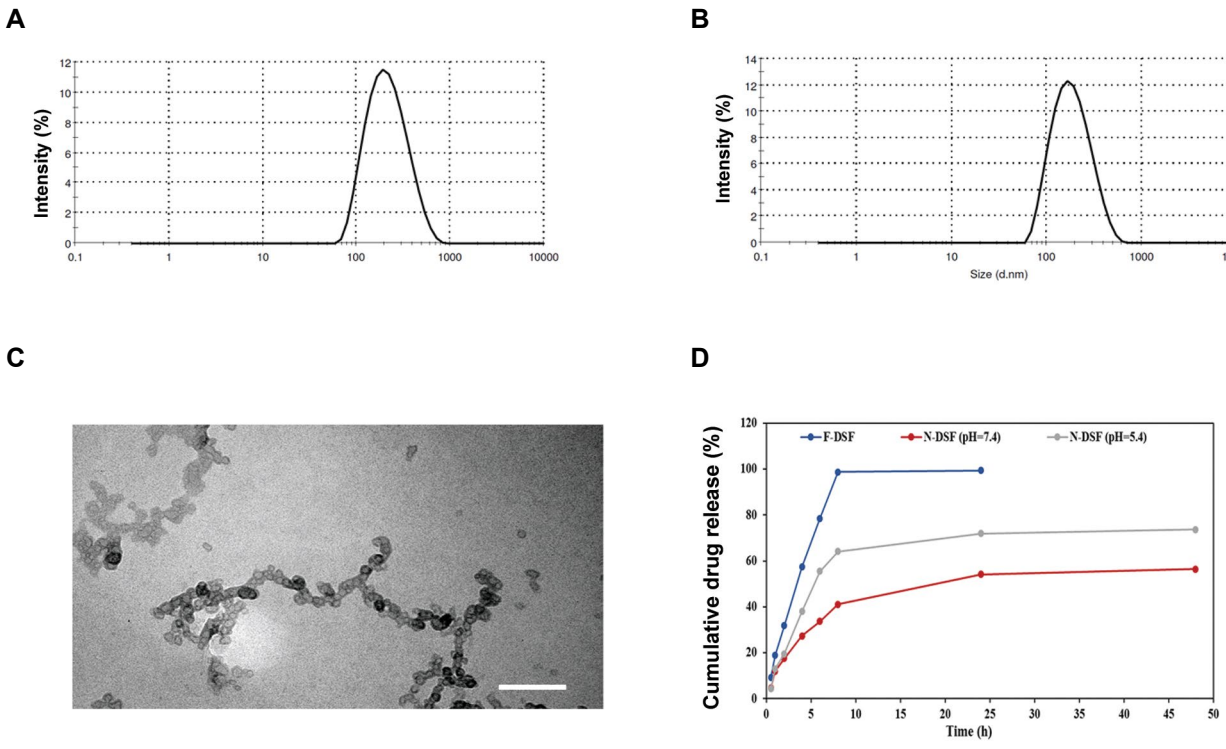

Fig.1: The particle size and PDI of **A.** Niosome-loaded DSF and **B.** Empty niosomes, **C.** TEM image of Niosome-loaded DSF (scale bar: 50µm), and **D.** DSF cumulative drug release from the niosomal formulation in different pH. PDI; Polidispercity index, DSF; Disulfiram, and TEM; Transmission electron microscopy.

Drug release kinetic model of different formulations

To demonstrate the mechanism of drug release from various formulations, the release kinetics of samples were examined after examining the drug release process in various formulations. According to the release data, various linear kinetic models were created. The kinetic model of sample release is represented by a model with a linear regression coefficient that is close to one. The release kinetics of DSF from the Niosomes forms are close to Korsmeyer-kinetic Peppa's model, as shown in Table 2D. This is likely because the drug dissolves slowly in the receptor phase of gradual release (19). The free medicines were discovered to adhere to the first-order kinetic model. The greater swelling and breaking of Niosomes in acidic circumstances is the cause of the different release kinetics.

A kinetic model with a recurrence ratio (R2) of 1 is suitable for formulations. According to the R2 of each model (Table 2D). The diffusion and erosion mechanisms control the drug release (20). The values obtained then represent Fickian diffusion drug release (0.43 n 0.85) (21). This was established by research on the manufactured niosomal formulations, which were only approximately stable without any significant changes for two weeks at a period with no additional time. However, samples kept at 42°C release less material more slowly because the Niosomes' membrane mobility is reduced at this temperature (22).

Table 2: Regression analysis, desirability criteria, RSM responses, and the kinetic release model

A. Results of regression analysis for responses

Response	**Size (nm)**	**PDI**	**EE (%) of DSF**
R-squared	0.9462	0.9211	0.9821
Adj R-squared	0.8924	0.8423	0.9643
Adeq precision	12.8825	10.8629	25.0208
Lack of fit	0.2724	0.5708	0.1358

B. Desirability criteria and predicted values for the variables

Number	**Lipid content (µM)**	**Surfactant per cholesterol, molar ratio**	**Desirability**
198.225	2	188.89	198.225

C. The optimized responses obtained by RSM and the experimental data for the same responses under the optimum conditions

Parameters	**Predicted**	**Experimental data**	
		N-DSF	**Empty Niosome (Nio)**
Particle size	188.89	189.7	164.4
PDI	0.183	0.187	0.17
EE (%) of DSF	80.1	79.3	-
Zeta potential (mV)	-	-20.4	-22.6

D. The kinetic release models and the parameters obtained for optimum N-DSF

Mathematical model	**Precision**	**Free DSF**	**Free DSF**	**N-DSF (pH=5.4)**
Zero	R2	0.4796	0.4796	0.7333
First	R2	0.9401	0.9401	0.5362
Higuchi	R2	0.6214	0.6214	0.8411
Korsmeyer-Peppa's	R2	0.7697	0.7697	0.9266
	n	0.5571	0.5571	0.5421

RSM; Response surface methodology, PDI; Polidispercity index, EE; Entrapment efficiency, and N-DSF; Disulfiram-loaded Niosomes.

DSF-loaded Niosomes inhibited cellular growth in OCC-11 cells

The data from the MTT-test analysis demonstrated that the drug's ideal dosage of 12.5 µg/ml solution of DSF-loaded Niosomes can inhibit cellular growth in comparison to the control group (P=0.0001, Fig.2A).

DSF- loaded Niosomes reduced colony formation capacity of OCC-11 cells

The results of the colony formation assay showed that the area of the colonies formed after treatment of the OCC-11 cells with DSF-loaded Niosomes was 60% lower in comparison to the free drug group, and 80% lower in comparison to the control group (P=0.0046, Fig.2B).

DSF- loaded Niosomes induced apoptosis in OCC-11 cells

The results of the flow cytometry test (Annexin V) indicated that DSF-loaded Niosomes increased the apoptosis rate in DSF-loaded Niosomes treated groups compared to the control groups (P=0.019, Fig.3).

Migration assay

As shown in the Figure 4, the migration capacity of the cells was reduced after drug treatment. Interestingly, these results suggested that after 72 hours treatment of the cells with DSF-loaded Niosomes, the migration ability were significantly declined in comparison to the control groups. (P=0.0015).

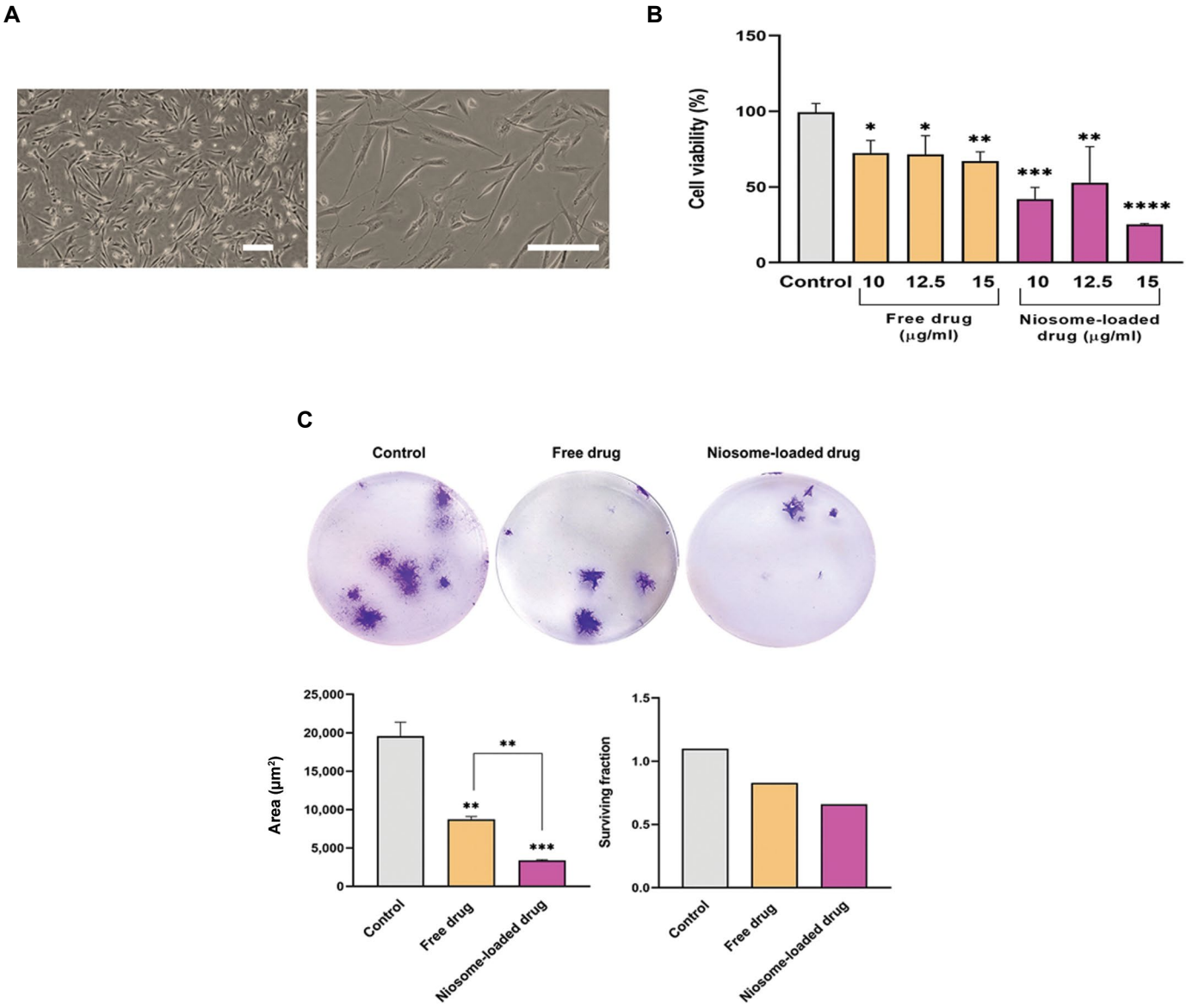

Fig.2: A. About 12.5 µg/ml solution of DSF-loaded Niosomes can inhibit cellular growth (P=0.0046). **B.** OCC-11 cells treated with DSF-loaded Niosomes developed 60% smaller colonies than the free drug group and 80% smaller colonies than the control group (scale bar: 100 µm). **C.** Colony formation assay. The area and the surviving fraction of emerged colonies in each group were quantified. DSF; Disulfiram, **; P≤0.01, and ***; P≤0.001.

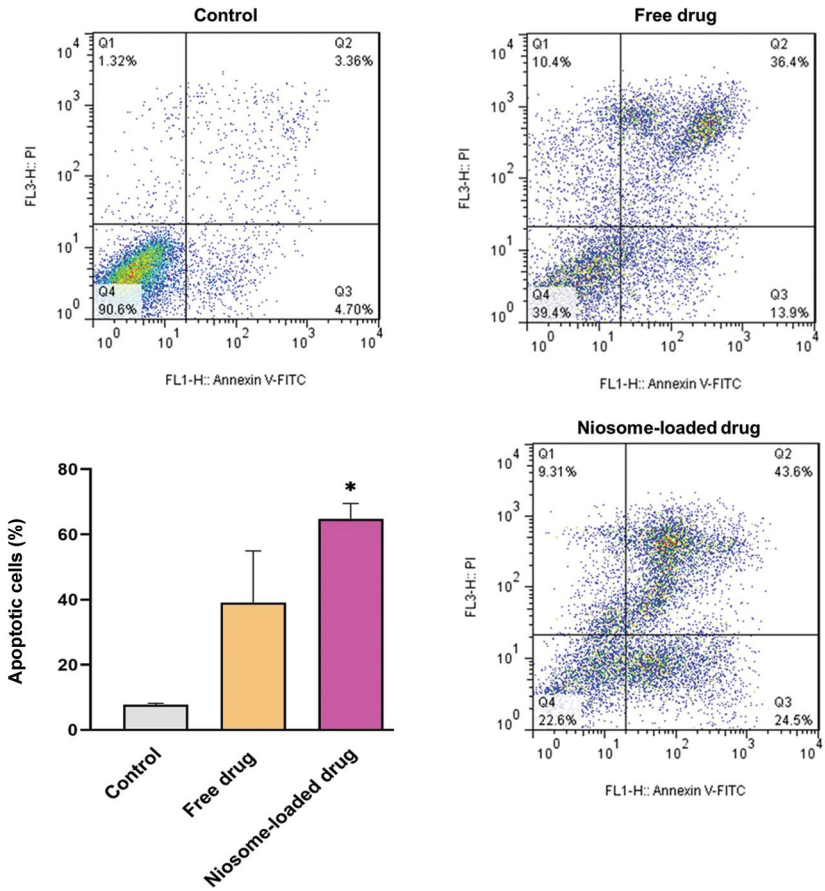

Fig.3: Data analysis of flow cytometry showed that DSF-loaded Niosome increased the apoptosis in the OSCC cells in comparison to control groups (P=0.019). DSF; Disulfiram and OSCC; Oral squamous cell carcinoma.

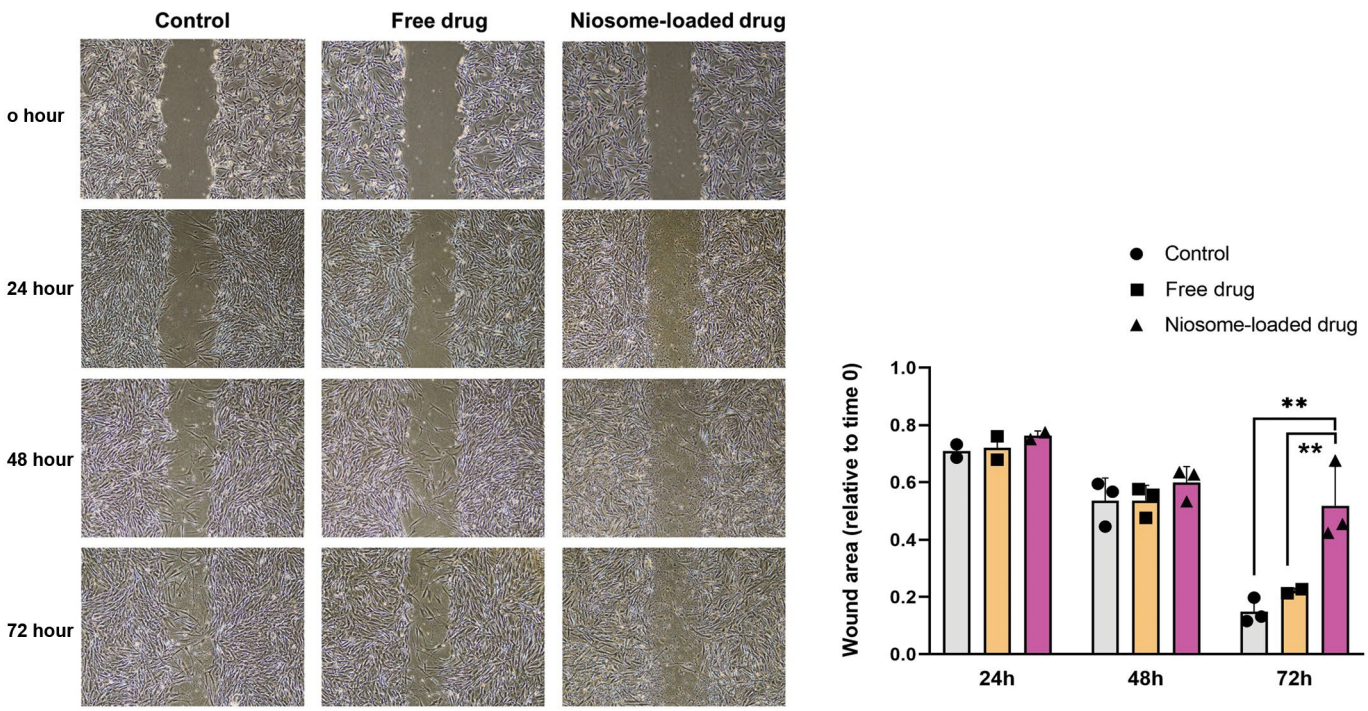

Fig.4: After 72 hours treatment of the cells with DSF-loaded Niosome, the migration capacity of the cells decreased significantly. DSF; Disulfiram and **; P=0.0015.

Discussion

Finding novel applications for currently available medications for cancer therapy can speed up the transition from laboratory research to clinical applications. In addition to their original medical indications, extensive efforts have been put to develop new applications for existing medications. One of the examples of a typical drug, which can be taken into practice in cancer targeted therapy is Disulfiram. DSF is used to treat alcoholism because it pharmacologically suppresses aldehyde dehydrogenase's (ALDH) enzyme activity. The patient has an uncomfortable sensation known as the "disulfiram response" as a result of the buildup of acetaldehyde. There is evidence indicating that inhibiting ALDH could reduce the "stemness" of cancer cells. In fact, numerous studies have shown that DSF has anti-cancer properties, mainly via inhibiting cancer stem cells and altering cellular communications (23). Evidence of DSF's anticancer activity has grown in recent years, which is currently being tested in several ongoing and some completed clinical trials. These studies examined the use of DSF for advanced solid tumors with metastases to the liver (24), metastatic melanoma (25), glioblastoma (26), and non-small cell lung cancer (28). Recent research supports the idea that DSF is well tolerated and can increase survival rate in patients with newly diagnosed non-small cell lung cancer (23).

The findings of our study support the earlier findings that treatment of OCC-11 cells with DSF-loaded Niosomes significantly reduced the number of emerged colonies. Results of the MTT test concurred with this data. This information indicated that in our migration test, the migration of the cells was reduced, and the DSF-loaded Niosomes could eliminate cell migration. We used primary cell line in our study, which is an advantage regarding that the characteristics of the cells are not genetically regulated.

In a xenograft mouse model, the effects of DSF on tumor growth and metastasis were investigated *in vivo*. Along with a decrease in the expression of epithelial-mesenchymal transition (EMT) markers in tumors, DSF also inhibited the development and spread of tumors *in vivo*. These findings suggested that DSF has broad-spectrum anticancer potential for clinical application against OSCC by inhibiting EMT in OSCC cells both *in vitro* and *in vivo* through Smad4 and regulation of the TGFβ- ERK-Snail pathway (9).

Farooq et al. (6) have shed a light on the fact that the pharmacological relevance and clinical applicability of DSF are limited despite its remarkable anticancer activity because of its poor stability, low solubility, short plasma half-life, quick metabolism, and fast clearance from systemic circulation. By enhancing its stability and preventing its degradation, nanotechnology-based interventions have received notable recognition for improving the pharmacokinetic and pharmacodynamic profile of DSF. Their comprehension of earlier literature supports the notion that the DSF nanomedicine, which is based on nanotechnology, is a sensible strategy for cancer therapy by specifically targeting cancer cells. The efficacy of different DSF nano-formulations in cellular studies emphasizes their potential for *in vivo* testing in animal models. Nanotechnology offers a revolutionary way for solving current challenges. The therapeutic potential, safety, and effectiveness of DSF have all enhanced when it is administered along with other chemo-toxic substances. Future nanomedicine-based DDs continue to look promising since they have the potential to improve cancer management. To better understanding the effectiveness and safety of DSF in clinical trials, more research must be done.

There is also supporting evidence of noisome-based treatments in rats with oral squamous cell carcinoma. Fazli et al. (3) aimed to ascertain the curcumin Niosomes effective dose in the culture and compare its prophylactic effect on oral cancer in rats when administered as mouthwash to that of its injectable form. First, free curcumin, curcumin-loaded Niosomes, and unloaded Niosomes were administered to KB oral cancer cells and human umbilical vein endothelial cells (HUVEC) in independent groups. Using injectable curcumin Niosomes was found to delay the onset of severe kinds of dysplasia in animal studies. Curcumin-loaded Niosomes prevented the emergence of severe forms of dysplasia and inhibited the growth of cancer cells.

Liposomes are sophisticated drug delivery technologies that are used in numerous pharmaceutical products with therapeutic focus. In the aqueous core of liposomes, McMahon et al. (28) created a nanoscale reactors to generate Cu (DDC) 2 complex NPs. In a nutshell, copper ion-loaded liposomes were first made. The copper ion-loaded liposomes were then combined with DDC. DDC entered the aqueous center of the liposomes through their membranes and formed a compound with copper ions there. This liposome-based technique successfully produced Cu (DDC) 2 NPs with outstanding anticancer efficacy in a mouse tumor model. To increase the targeting specificity of liposomes, tumor-targeted moieties can be added. Similar techniques were employed by Mareng et al. to make tumor-targeting Cu (DDC) 2 liposomes. They altered the liposomes' surface with hyaluronic acids in order to target pancreatic cancer stem cells that express the CD44 protein. The tumour growth was significantly inhibited by these liposomes.

Bartelds et al. (12) showed that Niosomes are a great alternative for liposomal drug delivery systems. They came to the conclusion that whereas permeability for tiny ions/solutes are higher, Niosomes have physicochemical properties that are similar to those of liposomes, making them potentially appealing candidate as drug carriers for a variety of compounds. Niosomes are less expensive and more stable than liposomes. The polydisperse nature of the commercially available surfactants (Spans and Tweens) is a drawback. Drug loading into the Niosomes has been done, and we demonstrated that freezing and

thawing resulted in losing their potency. Niosomes have been used in preliminary animal investigations, but no clinical trials have been published.

In the current study, a novel DSF-loaded niosomal formulation were fabricated. Particle size, PDI, and EE (%) of 11 different formulations of fabricated Niosomes were compared. EE (%) of nanoparticles improved by increasing the amount of cholesterol due to strengthening the nonpolar Niosomes' tail and amplifying the chain order of the liquid-state bilayer (3). Also, the optimization results showed that cholesterol improved bilayer membrane rigidity and enhanced the physical stability of nanoparticles (28). Other studies showed that by increasing the cholesterol concentration, the size of nanoparticles increased as well. Cholesterol molecules take up the membrane area, and surfactant polar heads occupy a smaller membrane area (29).

The size of optimum N-DSF evaluated by dynamic light scattering (DLS) and TEM was 189.7 and 40 nm, respectively. The Niosomes' size is significantly smaller when observed by TEM compared to the DLS. This difference is due to the TEM imaging drying process. In other words, the exact diameter and the hydrodynamic diameter of Niosomes observed by TEM and DLS, respectively. The hydrodynamic diameter means the size of particles with the core and any molecule attached or adsorbed surface (30). Same as other drug carriers, the DSF release profile is biphasic. An initial rapid release precedes the following slower release step. The initial fast release rate was regulated by diffusion. The drug's sustained release from the inner layer causes the later slow release. Also, the release of DSF was increased in acidic medium (31, 32). Tumors microenvironment is generally acidic, so the drug release rate from nanoparticles would be more higher in the vicinity of tumors than in healthy tissues (32).

Conclusion

In order to improve the efficacy of the treatment, this study came up with the niosomal drug delivery system, which in many aspects, overrates the other drug delivery system and can effectively reduce the toxicity rate and increase the half-life of the drug. DSF-loaded Niosomes have a controlled release pattern, which favours our treatment. Our findings revealed that DSF-loaded Niosomes increased apoptosis in the OSCC cells. In addition, colony formation capacity and migration ability of OSCC cells were decreased.

Acknowledgements

We would like to express our sincere gratitude to our colleagues at Royan Institute, Liver Research Group and Regenerative Medicine Department and Cell Culture Facility at Gastrointestinal Research Centre, SBUMS, Tehran, Iran. This study was funded by grants from Bahar Tashkhis Teb Co, (R.990017) and Royan Institute (R1399-9900075) and Tehran University of Medical Sciences, Dentistry Faculty, Department of Oral and Maxillofacial Pathology (TUMS-6897) There is no Conflict of interest in this study.

Authors' Contributions

M.Z.M.; Drafted the manuscript, did the experiments, and involved in data analysis. P.A., M.K., M.K.A., Z.M.-L., N.R.; Involved in producing Niosomes, experiments, reviewing manuscript and preparing figures. N.M., N.H.-K., M.V.; Involved in conceptualization, methodology, and reviewing manuscript. M.V., N.M.; Approved the final draft and financially supported the study. All authors read and approved the final manuscript.

References

1. Nagao T, Warnakulasuriya S. Screening for oral cancer: future prospects, research and policy development for Asia. Oral Oncol. 2020; 105: 104632.
2. Cristaldi M, Mauceri R, Di Fede O, Giuliana G, Campisi G, Panzarella V. Salivary biomarkers for oral squamous cell carcinoma diagnosis and follow-up: current status and perspectives. Front Physiol. 2019; 10: 1476.
3. Fazli B, Irani S, Bardania H, Moosavi MS, Rohani B. Prophylactic effect of topical (slow-release) and systemic curcumin nanoniosome antioxidant on oral cancer in rat. BMC Complement Med Ther. 2022; 22(1): 109.
4. Bugshan A, Farooq I. Oral squamous cell carcinoma: metastasis, potentially associated malignant disorders, etiology and recent advancements in diagnosis. F1000Res. 2020; 9: 229.
5. Liu L, Chen J, Cai X, Yao Z, Huang J. Progress in targeted therapeutic drugs for oral squamous cell carcinoma. Surg Oncol. 2019; 31: 90-97.
6. Farooq MA, Aquib M, Khan DH, Hussain Z, Ahsan A, Baig MMFA, et al. Recent advances in the delivery of disulfiram: a critical analysis of promising approaches to improve its pharmacokinetic profile and anticancer efficacy. Daru. 2019; 27(2): 853-862.
7. Yeung KT, Yang J. Epithelial-mesenchymal transition in tumor metastasis. Mol Oncol. 2017; 11(1): 28-39.
8. Bu W, Wang Z, Meng L, Li X, Liu X, Chen Y, et al. Disulfiram inhibits epithelial-mesenchymal transition through TGFβ-ERK-Snail pathway independently of Smad4 to decrease oral squamous cell carcinoma metastasis. Cancer Manag Res. 2019; 11: 3887-3898.
9. Rezaei N, Akbarzadeh I, Kazemi S, Montazeri L, Zarkesh I, Hossein-Khannazer N, et al. Smart materials in regenerative medicine. Mod Med Lab J. 2021; 4(1): 39-51.
10. Akbarzadeh I, Farid M, Javidfar M, Zabet N, Shokoohian B, Arki MK, et al. The optimized formulation of tamoxifen-loaded niosomes efficiently induced apoptosis and cell cycle arrest in breast cancer cells. AAPS PharmSciTech. 2022; 23(1): 57.
11. Akbarzadeh I, Fatemizadeh M, Heidari F, Niri NM. Niosomal formulation for co-administration of hydrophobic anticancer drugs into MCF-7 cancer cells. Arch Adv Biosci. 2020; 11(2): 1-9.
12. Bartelds R, Nematollahi MH, Pols T, Stuart MCA, Pardakhty A, Asadikaram G, et al. Niosomes, an alternative for liposomal delivery. PLoS One. 2018; 13(4): e0194179.
13. Rezaei N, Kazem Arki M, Miri-Lavasani Z, Solhi R, Khoramipour M, Rashedi H, et al. Co-delivery of doxorubicin and paclitaxel via noisome nanocarriers attenuates cancerous phenotypes in gastric cancer cells. Eur J Pharm Biopharm. 2023: S0939-6411(23)00102-9.
14. Rochani AK, Balasubramanian S, Ravindran Girija A, Raveendran S, Borah A, Nagaoka Y, et al. Dual mode of cancer cell destruction for pancreatic cancer therapy using Hsp90 inhibitor loaded polymeric nano magnetic formulation. Int J Pharm. 2016; 511(1): 648-658.
15. Alemi A, Zavar Reza J, Haghiralsadat F, Zarei Jaliani H, Haghi Karamallah M, Hosseini SA, et al. Paclitaxel and curcumin coadministration in novel cationic PEGylated niosomal formulations exhibit enhanced synergistic antitumor efficacy. J Nanobiotechnology. 2018; 16(1): 28.
16. Jaya Prakash N, Shanmugarajan D, Kandasubramanian B, Khot P, Kodam K. Biodegradable silk-curcumin composite for sustained drug release and visual wound monitoring. Mater Today Chem.

2023; 27: 101289.
17. Karimifard S, Rezaei N, Jamshidifar E, Moradi Falah Langeroodi S, Abdihaji M, Mansouri A, et al. PH-responsive chitosan-adorned niosome nanocarriers for co-delivery of drugs for breast cancer therapy. ACS Appl Nano Mater. 2022; 5(7): 8811-8825.
18. Franken NA, Rodermond HM, Stap J, Haveman J, van Bree C. Clonogenic assay of cells in vitro. Nat Protoc. 2006; 1(5): 2315-2319.
19. Pourtalebi Jahromi L, Ghazali M, Ashrafi H, Azadi A. A comparison of models for the analysis of the kinetics of drug release from PLGA-based nanoparticles. Heliyon. 2020; 6(2): e03451.
20. Heredia NS, Vizuete K, Flores-Calero M, Pazmiño VK, Pilaquinga F, Kumar B, et al. A. Comparative statistical analysis of the release kinetics models for nanoprecipitated drug delivery systems based on poly(lactic-co-glycolic acid). PLoS One. 2022; 17(3): e0264825.
21. Sadeghi S, Ehsani P, Ahangari Cohan R, Sardari S, Akbarzadeh I, Bakhshandeh H, et al. Design and physicochemical characterization of lysozyme loaded niosomal formulations as a new controlled delivery system. Pharm Chem J. 2020; 53(10): 921-930.
22. Damera DP, Nag A. Tuning the phase transition temperature of hybrid Span60-L64 thermoresponsive niosomes: Insights from fluorescence and Raman spectroscopy. J Mol Liq. 2021; 340(17): 117110.
23. Jiao Y, Hannafon BN, Ding WQ. Disulfiram's anticancer activity: evidence and mechanisms. Anticancer Agents Med Chem. 2016; 16(11): 1378-1384.
24. Kelley KC, Grossman KF, Brittain-Blankenship M, Thorne KM, Akerley WL, Terrazas MC, et al. A phase 1 dose-escalation study of disulfiram and copper gluconate in patients with advanced solid tumors involving the liver using S-glutathionylation as a biomarker. BMC Cancer. 2021; 21(1): 510.
25. Meraz-Torres F, Plöger S, Garbe C, Niessner H, Sinnberg T. Disulfiram as a therapeutic agent for metastatic malignant melanoma-old myth or new logos? Cancers (Basel). 2020; 12(12)3538.
26. Jakola AS, Werlenius K, Mudaisi M, Hylin S, Kinhult S, Bartek J Jr, et al. Disulfiram repurposing combined with nutritional copper supplement as add-on to chemotherapy in recurrent glioblastoma (DIRECT): Study protocol for a randomized controlled trial. F1000Res. 2018; 7: 1797.
27. Paller CJ, Antonarakis ES. Management of biochemically recurrent prostate cancer after local therapy: evolving standards of care and new directions. Clin Adv Hematol Oncol. 2013; 11(1): 14-23.
28. McMahon A, Chen W, Li F. Old wine in new bottles: advanced drug delivery systems for disulfiram-based cancer therapy. J Control Release. 2020; 319: 352-359.
29. Patel J, Ketkar S, Patil S, Fearnley J, Mahadik KR, Paradkar AR. Potentiating antimicrobial efficacy of propolis through niosomal-based system for administration. Integr Med Res. 2015; 4(2): 94-101.
30. Huang X, Liao W, Zhang G, Kang S, Zhang CY. pH-sensitive micelles self-assembled from polymer brush (PAE-g-cholesterol)-b-PEG-b-(PAE-g-cholesterol) for anticancer drug delivery and controlled release. Int J Nanomedicine. 2017; 12: 2215-2226.
31. Akbari V, Abedi D, Pardakhty A, Sadeghi-Aliabadi H. Release studies on ciprofloxacin loaded non-ionic surfactant vesicles. Avicenna J Med Biotechnol. 2015; 7(2): 69-75.
32. Akbarzadeh I, Rezaei N, Bazzazan S, Mezajin MN, Mansouri A, Karbalaeiheidar H, et al. In silico and in vitro studies of GENT-EDTA encapsulated niosomes: A novel approach to enhance the antibacterial activity and biofilm inhibition in drug-resistant Klebsiella pneumoniae. Biomater Adv. 2023; 149: 213384.